Supporting Online Material for

Clr4/Suv39 and RNA Quality Control Factors Cooperate to Trigger RNAi and Suppress Antisense RNA

Ke Zhang, Tamas Fischer, Rebecca L. Porter, Jothy Dhakshnamoorthy, Martin Zofall, Ming Zhou, Timothy Veenstra, Shiv I. S. Grewal*

*To whom correspondence should be addressed. E-mail: grewals@mail.nih.gov

Published 25 March 2011, *Science* **331**, 1624 (2011)
DOI: 10.1126/science.1198712

This PDF file includes:

Table S1
Two-hybrid screening for Clr4-interacting factors identify Mlo3 protein

Total clones screened	Screened clones		Sequenced clones	Mlo3 clones
	Ade^+His^+	Ade^+His^+ Mel^+		
>2 $X10^6$	63	15	20	10
	15	5		

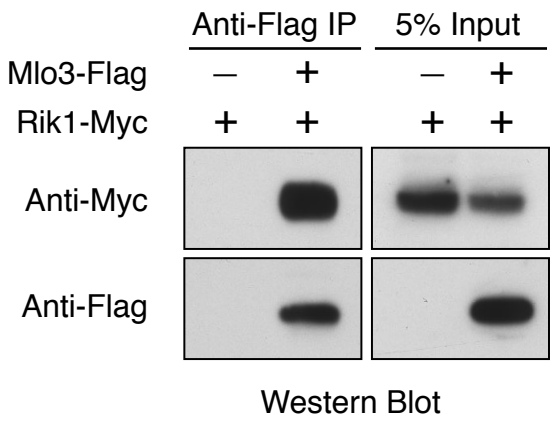

Figure S1. ClrC component Rik1 interacts with Mlo3. IP using anti-Flag antibody was followed by Western blot with anti-Myc antibodies. A longer exposure time was used to obtain the image shown for the anti-Myc input blot compared to that of IP blot.

Figure S1

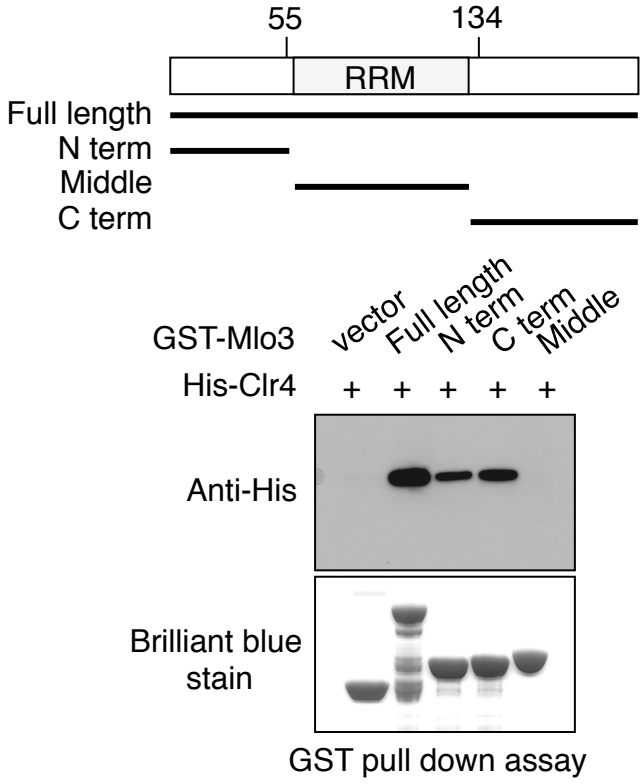

Figure S2. Clr4 interacts with Mlo3 in vitro. His-Clr4 GST pull-down assay using full-length or truncated Mlo3 proteins was followed by Western analysis using anti-His antibody to detect the presence of His-Clr4 or brilliant blue staining to visualize the GST fusion proteins. Schematic diagram shows various Mlo3 domains. GST fusions of Mlo3 are indicated. N-term: amino-terminal (1-55aa), C-term: carboxy-terminal (134-199aa); Middle: the RRM domain (56-134aa) and Vector: GST alone.

Figure S2

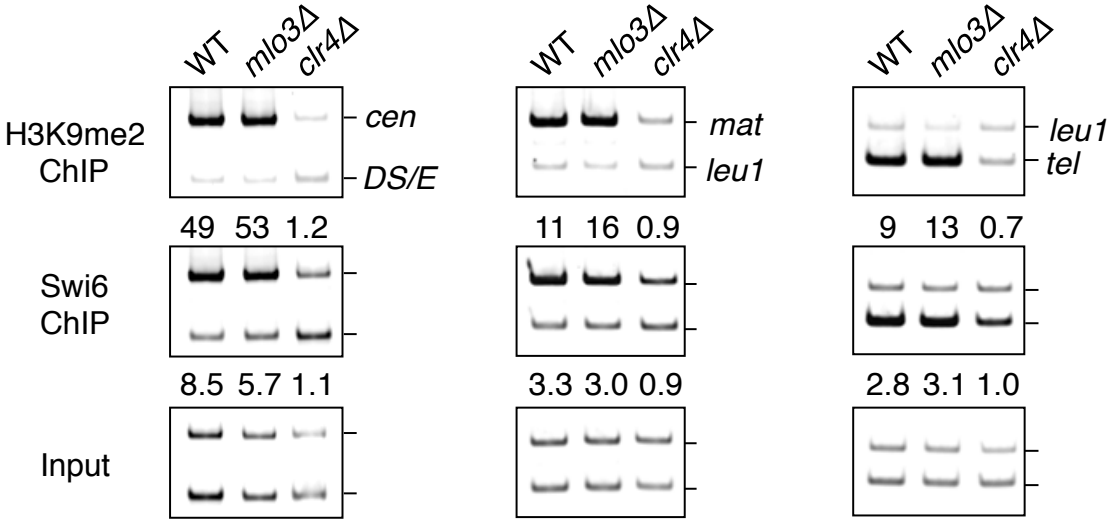

Figure S3. *mlo3Δ* cells maintain H3K9me2 and Swi6 localization at centromeres, mating type locus and subtelomeric loci. DNA isolated from ChIP and whole cell extract (Input) was analyzed by multiplex PCR, with primers designed to amplify *ura4*$^{+}$ inserted at centromere 1 (*cen*), the mating type locus (*mat*) or subtelomeric region (*tel*) and the internal control corresponding to a euchromatic gene (DS/E or *leu1*).Relative enrichment (shown below each lane) was calculated by dividing the intensity ratio of bands corresponding to heterochromatic and control euchromatic loci in the ChIP sample with those of input.

Figure S3

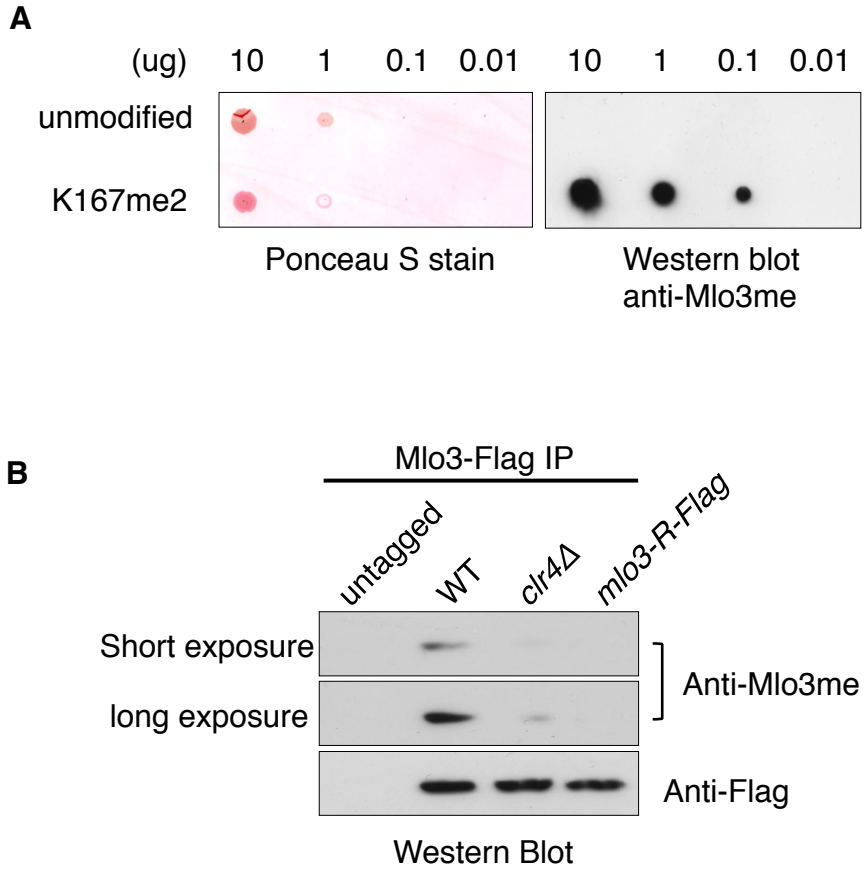

Figure S4. Detection of Mlo3 methylation in vivo. (**A**) Western blot using affinity purified anti-Mlo3me was performed to detect unmodified or methylated Mlo3 peptides serially diluted and spotted onto nitrocellulose membrane. Poncean S stain show the loading of peptides. (**B**) Flag tagged Mlo3 was immunoprecipitated using conjugated Flag agarose from indicated yeast strain extracts. Western blots were performed using anti-Flag antibody as the loading control (bottom) or using anti-Mlo3me to detect methylated Mlo3. *mlo3-R-Flag*: *mlo3K165RK167R-Flag*

Figure S4

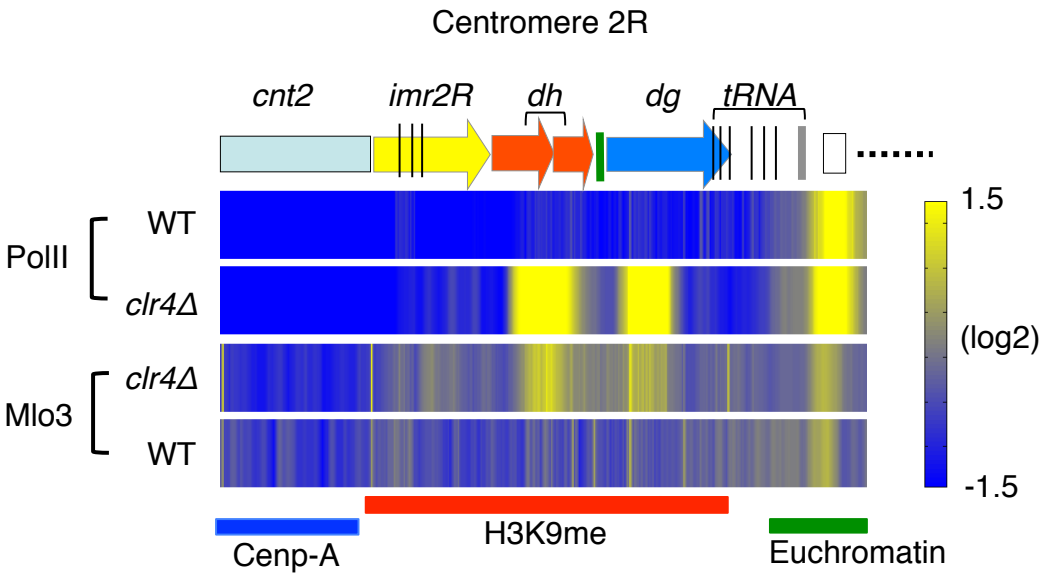

Figure S5. Mlo3 localization at pericentromeric *dg* and *dh* repeat elements. Heat map indicating levels of Pol II and Mlo3-Flag in wild type (WT) or *clr4Δ* cells determined by ChIP-chip are shown in alignment with the physical map of the right region of centromere 2 (centromere 2R). The centromere 2R is annotated according to 2004 *S. pombe* Sanger Center database release. Red, green and blue lines at bottom indicate pericentromeric heterochromatic regions enriched for methylated H3K9 (H3K9me), euchromatic region and central core region containing Cenp-A, respectively.

Figure S5

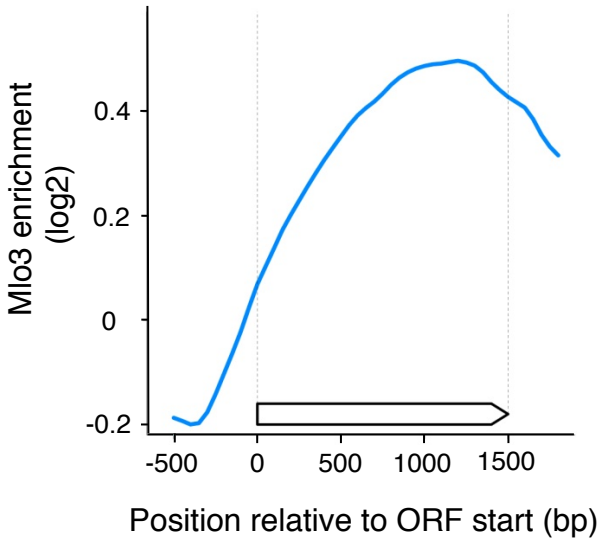

Figure S6. Mlo3 is enriched at genes with the peak toward the 3' end of ORF. ORFs were divided into 30 equally sized segments. Geometric averages of the corresponding segments between ORFs were calculated and plotted as average enrichments over a 50bp region. 0 in X-axis represents the beginning of the ORF, and 1500 bp represents the end of the ORF. Y axis shows the average enrichment in log2 scale.

Figure S6

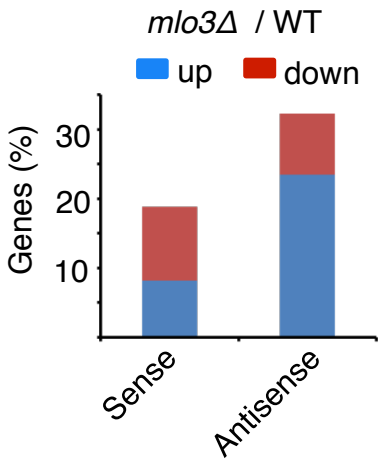

Figure S7. Sense and antisense transcriptome analysis in *mlo3Δ* mutant cells. The percentage of genes with at least 2-fold altered mean transcript levels in *mlo3Δ* cells, as compared to wild-type cells was plotted.

Figure S7

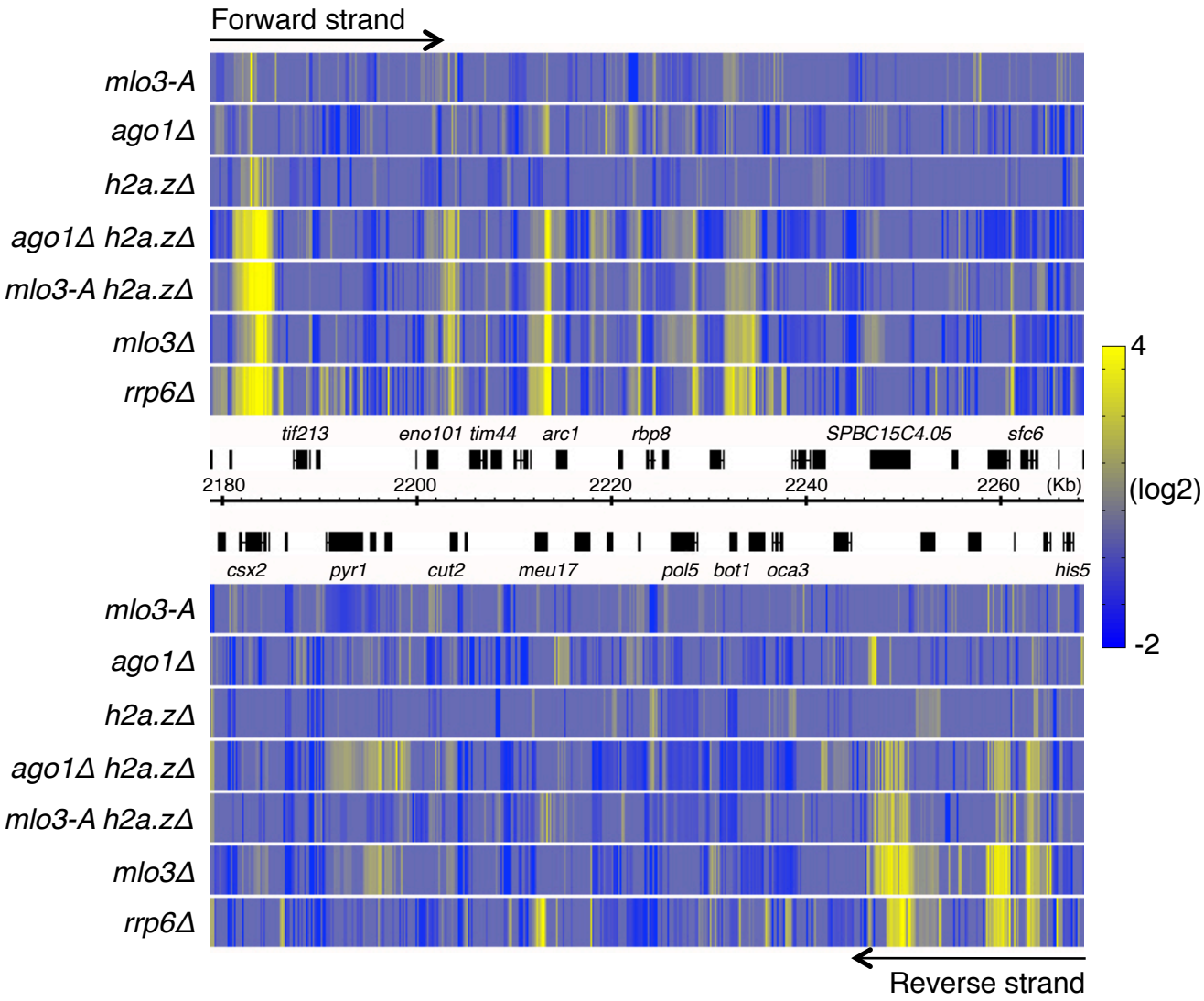

Figure S8. Representative genomic regions with elevated antisense transcripts in indicated mutants. Expression profiling was performed using high density tiling microarray. The increase in levels of antisense RNA is shown by the heat map. Forward transcripts are shown on top, and reverse transcripts are shown on the bottom. Relative expression values (mutants as indicated / WT) were converted into color gradient.

Figure S8

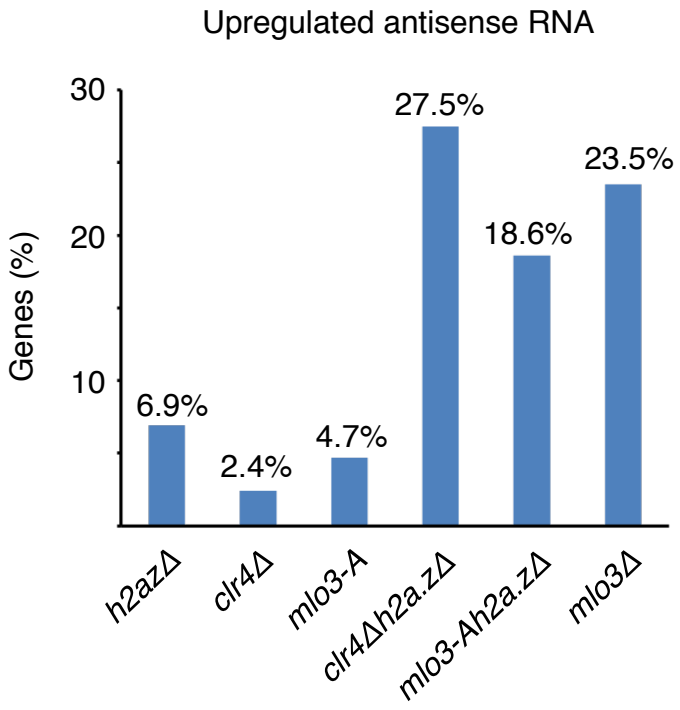

Figure S9. Levels of antisense RNA in single and double mutants. Upregulated antisense RNA was estimated as a percentage of genes (%) shown on the top of each bar representing the indicated strains.

Figure S9

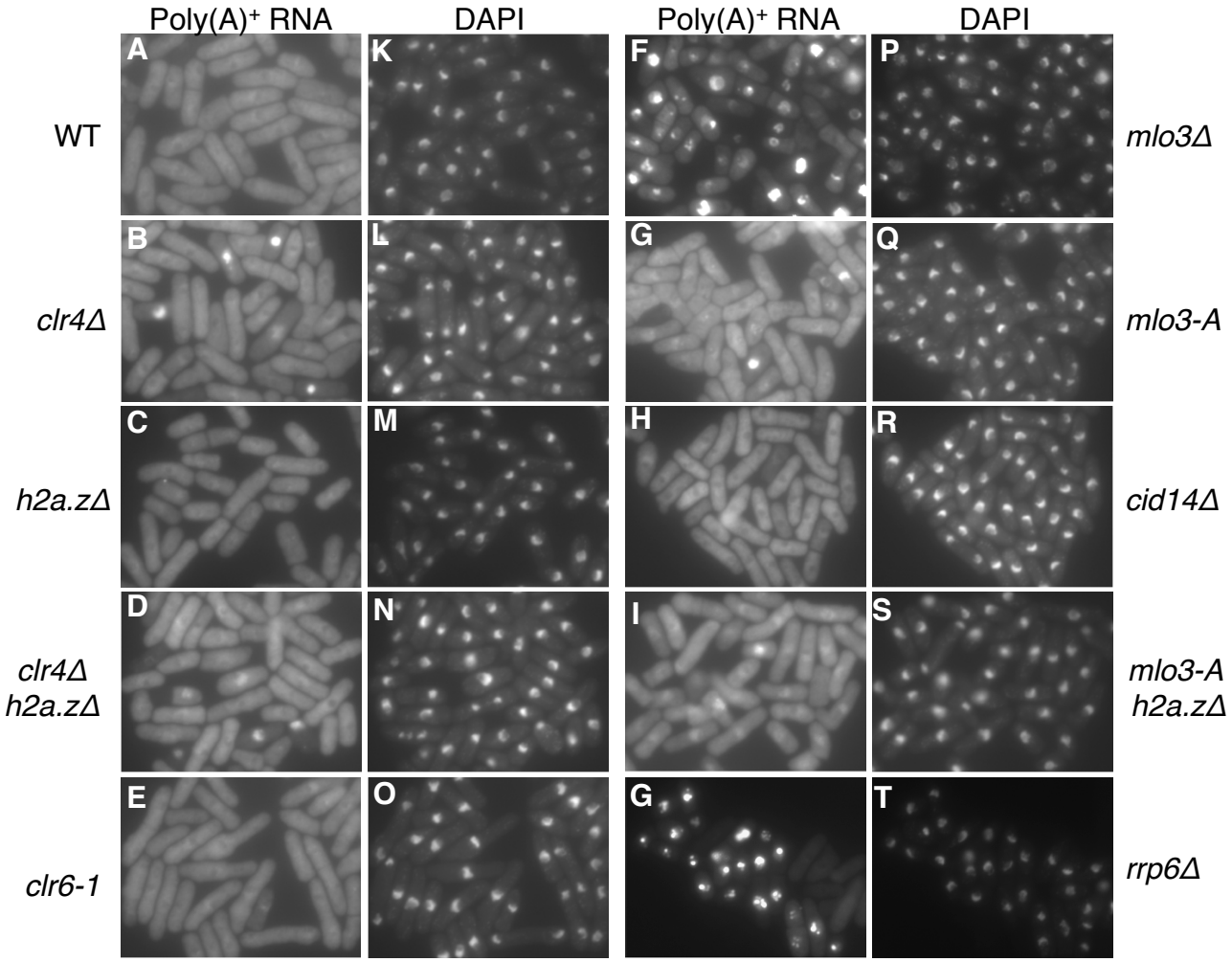

Figure S10. *clr4Δ and mlo3-A* mutants similarly show nuclear accumulation of poly(A)+ RNA. In situ hybridization of poly(A)+ RNA in indicated strains is shown (**A-G).** The corresponding right panel (**K-T**) show DAPI-stained nuclei. *clr4Δh2a.zΔ* (**D**) or *mlo3-Ah2a.zΔ* (**I**) mutants, which show highly elevated levels of antisense RNA, do not display corresponding increase in poly(A)+ RNA in the nucleus. Moreover, deletion of Cid14 subunit of TRAMP or a mutation in Clr6 histone deacetylase, which is known to cause global increase in acetylation of histones and elevated levels of antisense transcripts originating from cryptic promoters, is not associated with nuclear accumulation of poly(A)+ signal. *rrp6Δ* cells (**G**) also accumulate poly(A)+ RNA in the nucleus in a manner similar with *mlo3Δ* cells (**F**). The phenotypic similarity between *rrp6Δ* and *mlo3Δ* may be due to defects in RNA export and/or in degradation of aberrant RNA.

Figure S10

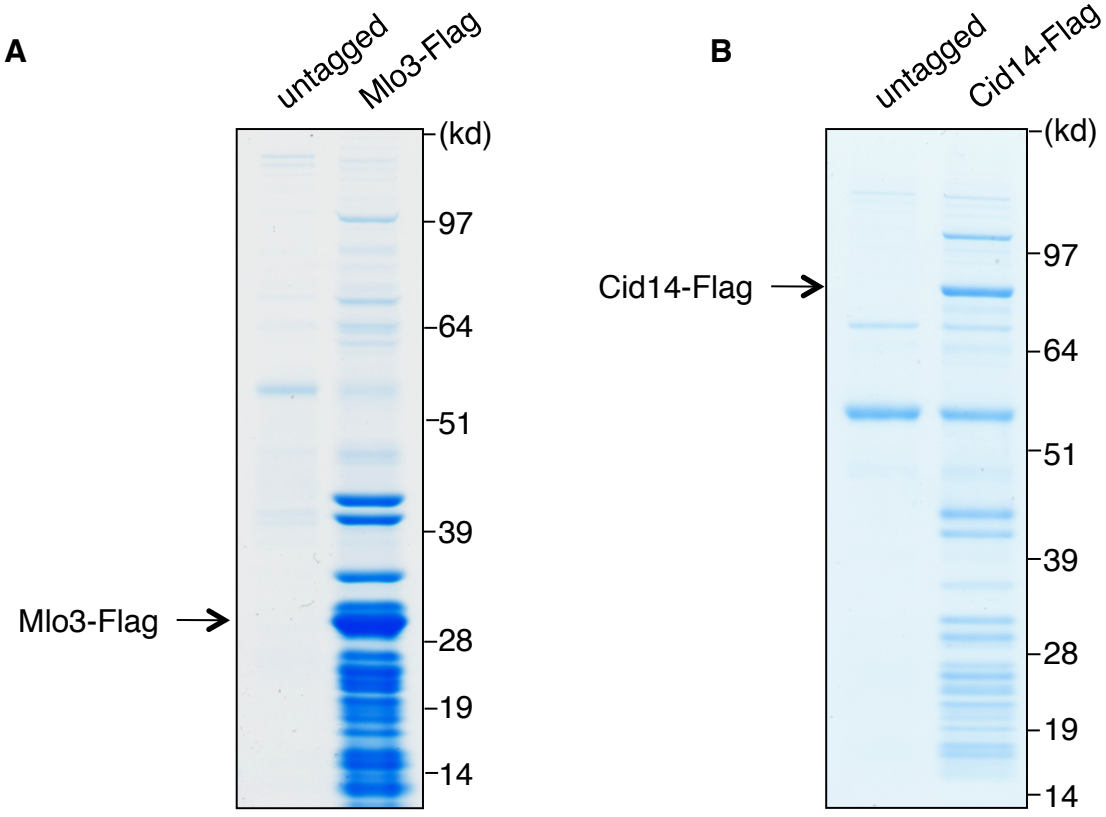

Figure S11. Purification of Mlo3-Flag and Cid14-Flag associated proteins. Brilliant blue stained 4-12% NuPAGE gels showing the purification of Mlo3-Flag (**A**) and Cid14-Flag (**B**) with their control purification from an untagged strain. The gel running position of Flag-tagged protein used for each purification is indicated.

Figure S11

Table S2

List of proteins identified in Mlo3-Flag purification

Gene Name	No. of amino acids recovered	Coverage (%)
Mlo3	161	80.90
Mtr4	114	16.67
Cid14	55	4.92
Air1	29	9.27
H4	39	37.86
Sal3	347	31.69
SPCP1E11.11	167	26.01
Nog1	160	24.92
Sik1	118	23.74
SPAC22G7.05	140	23.41
SPCC126.11c	42	22.95
Ebp2	72	21.62
Nop58	109	21.46
H2B	27	21.43
Srp2	71	19.45
SPBC4F6.13c	140	19.02
ppp1	111	18.29
pescadillo-family	53	17.79
Sla1	23	17.42
H2A	61	16.53
Rnp24	51	16.09
Rpf2	97	15.25
Ded1	62	13.08
Upf1	119	12.86
H3	17	12.50
Brx1	35	11.86
Nop12	51	11.64
Pwp1	59	11.43
Noc1	95	11.05
SPBC4F6.14	74	10.98
Rrs1	18	10.84
SPCC16C4.16c	17	10.56
Has1	61	10.55
Cic1	37	9.92
Noc2	59	8.35
Nop52	17	7.83
Utp23	19	7.31
Gar1	13	6.70
Mak16	18	5.96
Gtp1	20	5.49
Utp21	48	5.32
Exo2	69	5.20

Ribosomal proteins and proteins with less than 5% sequence coverage are not included in the list

Table S3

List of proteins identified for Cid14-Flag purification

Gene Name	No. of amino acids recovered	Coverage (%)
Cid14	563	82.31
Mtr4	779	69.74
Air1	158	50.48
Mlo3	153	76.88
Rpf2	138	43.53
UPF0462	45	38.46
H2B	45	35.71
Nog1	212	33.02
Sla1	97	32.55
Dbp2	179	32.55
Rlp24	56	29.17
H4	30	29.13
Brx1	74	25.08
Srp2	90	24.66
Nop53 (rrp16)	103	24.58
H2A	30	22.73
eIF4G	318	22.67
Puf6	143	22.27
eIF6	54	22.13
Ded1	136	21.38
Sik1	96	19.32
Grn1	90	19.15
notchless-like protein	95	18.92
ribosome export GTPase	100	18.62
Ebp2	62	18.62
Rnp24	67	18.16
Sec65	35	17.59
SPCC126.11c	31	16.94
Nsa2	42	16.15
Rrp15	33	16.10
Rrs1	26	15.66
Nop58	79	15.55
eIF2 beta	49	15.26
eIF2alpha	44	14.38
Nob1	53	13.66
eIF2gamma	59	13.23
eIF5A	18	11.46
Tho complex	31	11.31
Fmp31	19	11.11
SPAC8F11.04	41	10.99
Rrp5	178	10.53
DNA polymerase V	95	9.91

Table S3 continue

List of proteins identified for Cid14-Flag purification

Gene Name	No. of amino acids recovered	Coverage (%)
SPBC4F6.13c	72	9.78
Nop2	54	8.88
Ytm1	39	8.86
SPAC10F6.08c (Ino80 subunit)	30	8.80
Cwf9	10	8.70
eIF3a	78	8.37
Sce3	32	8.25
EF-1 beta	17	7.94
H3.1/H3.2	10	7.35
Far10	22	7.31
Nop12	31	7.08
NIFK	19	6.88
Sum1	22	6.71
Gar1	13	6.70
SPBC16A3.08c	19	6.69
Utp15	32	6.48
Fnx1	34	6.40
eIF3c	55	5.99
SPBC4F6.14	40	5.93
Ppk9	31	5.83
SPAC1093.04c	28	5.60
SPBC16H5.08c	34	5.50
Rec24	19	5.43
SPBC16H5.12c	37	5.43
Spb1	43	5.36
SPCC736.12c	23	5.26
SPBC365.04c	12	5.15

Ribosomal proteins and proteins with less than 5% sequence coverage are not included in the list

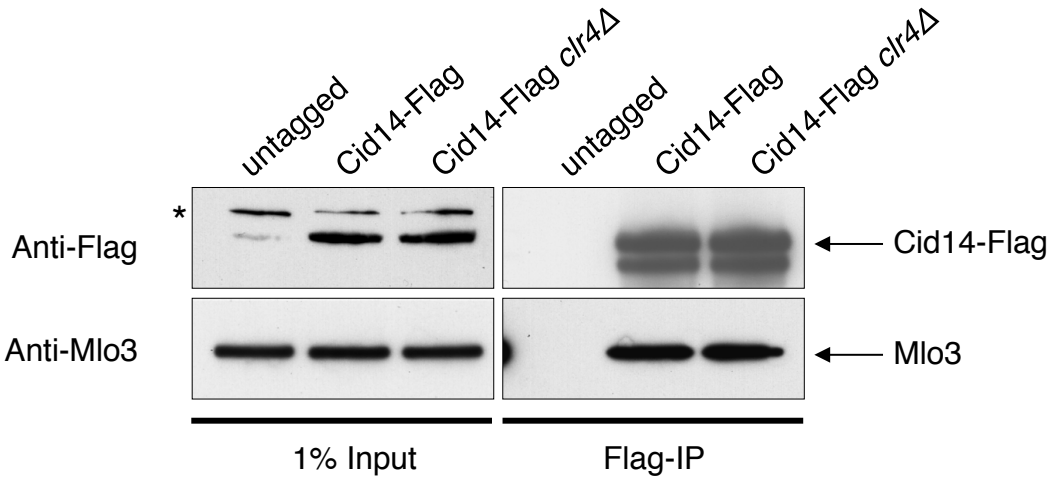

Figure S12. The interaction between Mlo3 and TRAMP is not affected by deletion of Clr4. IP from indicated strains using anti-Flag antibody was followed by Western blot with Mlo3 antibody. A longer exposure time was used to obtain the image shown for the anti-Flag input blot compared to that of IP blot. Asterisks indicate nonspecific bands.

Figure S12

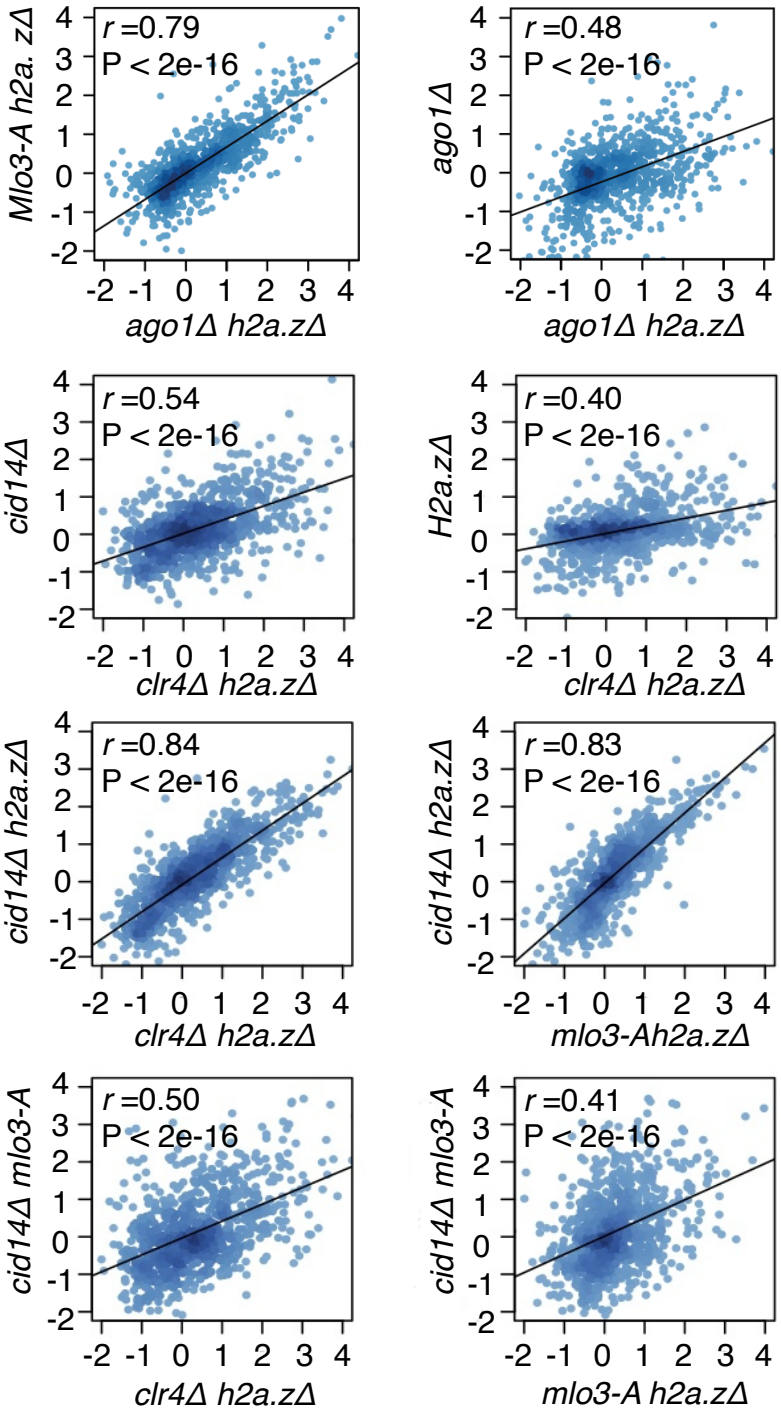

Figure S13. Mlo3 suppresses antisense RNA at loci targeted by Clr4, RNAi and TRAMP. Density plots comparing the upregulation of antisense transcripts in indicated mutants over wild type cells. Pearson's correlation coefficient (*r*) and the *P* value of the linear regression for each pair are indicated.

Figure S13

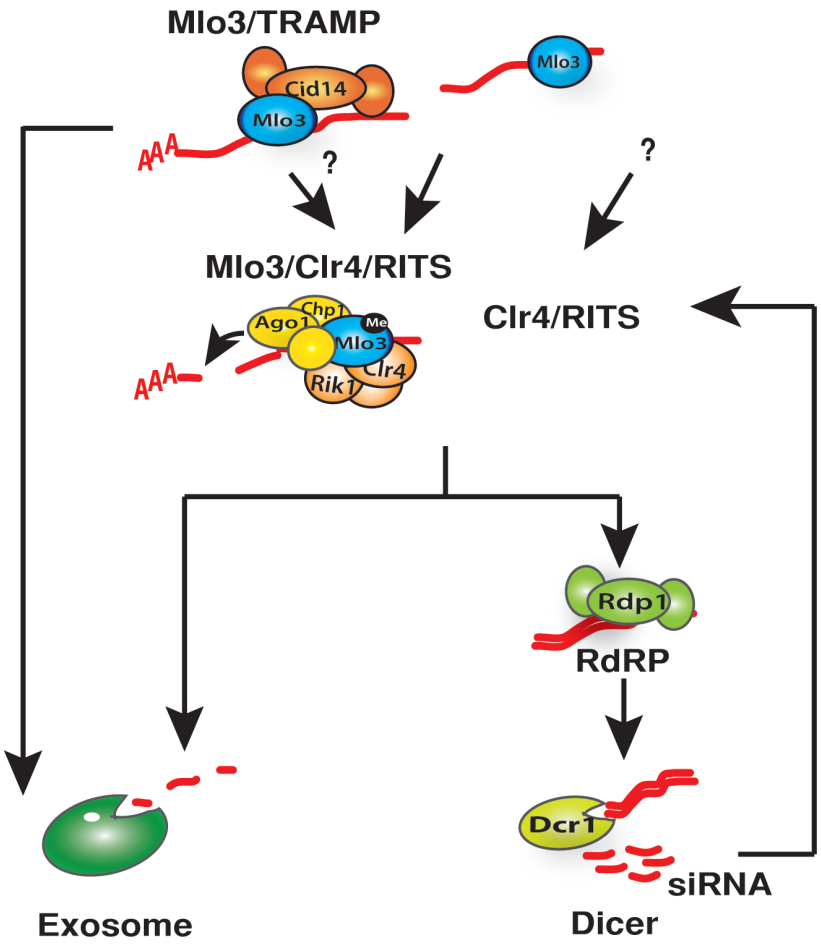

Figure S14. Model showing processing of centromeric and antisense RNA by the coordinated action of Mlo3, TRAMP, Clr4, RNAi and the exosome. Centromeric and antisense RNAs are recognized by Mlo3 and/or Mlo3/TRAMP, which presumably tags transcripts for degradation via its polyadenylation activity. RNA targeted by Mlo3/TRAMP can be degraded directly by the exosome. Mlo3 also feeds RNAs into RNAi pathway via mechanism involving Clr4 that facilitates the interaction between Mlo3 and RITS. Clr4 also methylates H3K9 (not shown) and Mlo3 which could independently influence loading of RNA processing activities including RNAi factors to the sites of aberrant RNA production and/or facilitate the recognition of transcripts marked for degradation. Since siRNAs can be detected in *mlo3Δ* cells, it is likely that alternative mechanism(s) exist that targets RNAi machinery to centromeric RNAs. RNA substrates targeted by the Ago1/RITS are either processed via RNA-dependent RNA polymerase and Dicer to generate siRNA, or are degraded by 3'-5' exonuclease activity of the exosome.

Figure S14

Online Materials and Methods

Fission Yeast strains and plasmids

mlo3-HA, *mlo3-Flag*, *mlo3Δ*, and *cid14-Flag* strains were constructed with a PCR based method. To generate *mlo3* mutant strains, a PCR fragment containing *mlo3-Flag::KanMX* was cloned into pCR-Blunt II-TOPO vector (Invitrogen) to construct pCR-TOPO- mlo3-(3X)Flag::KanMX. Site-directed mutagenesis was used to introduce mutations into cloned *mlo3* using Quickchange^{TM} protocols (Stratagene). The mutant alleles were then introduced into yeast by transforming a PCR fragment containing the mutant mlo3-(3X)Flag-kanMX cassette into a wild type strain and selecting for G418 positive colonies, which were subjected to DNA sequencing to confirm proper insertion of mutant *mlo3-Flag*. The plasmids used for expression of GST-Mlo3 were made previously (*1*). Site-directed mutagenesis of GST-Mlo3 was carried out using Quickchange^{TM} protocols (Stratagene). The construction of *Flag-Clr4*, *cid14Δ*, *Rik1-Myc* strains used in this study was described previously (*2-3*). Standard genetic crosses were employed to construct all other strains. Yeast cells were grown according to standard procedures.

Yeast-two hybrid screening

The coding sequence of Clr4 was PCR amplified and cloned into pGBKT7 (Clontech) to generate the bait plasmid pGBKT7-Clr4. The bait plasmid was transformed into the *S. cerevisiae* Y190 strain (*MATa ura3-52 his3-D200 lys2-801 ade2-101 typ1-901 leu2-3 112gal4Dgal80D LYS2::GAL-lacZ cyh^{r}*). The presence of bait plasmid alone in Y190 does not activate reporter genes (data not shown). *S. pombe* cDNA library based on pGAD-GH (Clontech) was transformed into pGBKT7-Clr4 containing Y190 cells. Positive colonies were selected by plating the transformed cells on SD-HIS-LEU-TRP plates and assayed for β−galactosidase activity according to the manufacturer's instructions. Genomic DNA was isolated from positive colonies, and transformed into *E. coli*. The plasmids recovered from *E. coli* were subjected to DNA sequencing to identify the potential Clr4 binding factors.

GST-pull down assay

Recombinant His-Clr4 and GST-Mlo3 were expressed in *E.coli* and purified as previously

described (*1, 4*). Binding assays were performed by incubation of 2-5 μg of purified proteins with Glutathione Sepharose^{TM}4B (GE healthcare) in 500 μl GST binding buffer (1xPBS plus 0.5 mM EDTA, 0.5% Np40, 1mM DTT and extra 100 mM NaCl) at 4^{o}C for 2hr. The beads were washed four times with GST binding buffer, and the bound proteins were eluted by boiling the beads in 30μl 1x SDS loading buffer. Pulled down fractions were analyzed by Western blot analysis.

***In vitro* methyltransferase assay**

Approximately 5μg of purified GST-Mlo3 or His-tagged H3 was incubated with 1μCi of *S*-adenosyl-L-[methyl-^{3}H]methionine (^{3}H-AdoMet; 15 Ci/mmol; GE Healthcare) and 2 μg of recombinant His-Clr4 protein in 20 μl of MTase buffer (50 mM Tris pH 8.0, 20 mM KCl, 10 mM $MgCl_2$, 1 mM DTT, 250 mM sucrose) for 1 hr at 30°C. The reactions were quenched by addition of 5 μl of 4X SDS loading buffer followed by boiling. The reaction was analyzed by SDS-PAGE and visualized by Brilliant Blue staining and fluorography.

Peptide synthesis and generation of anti-Mlo3me antibody

Peptides corresponding to amino acid 161-174 in Mlo3 containing unmodified or dimethyl lysine were synthesized by GenScript. The same peptides were used to raise polyclonal rabbit antiserum and to perform affinity purification of antibody.

ChIP, ChIP-chip and expression profiling

ChIPs and ChIP-chip analyses were performed as described previously with antibodies against Swi6, dimethylated H3K9 (Abcam) and Flag M2 (Sigma) (*3, 5*). The expression profiling was carried out according to a protocol described previously (*3*). In conventional ChIP assays, enrichment values shown below lanes were calculated by dividing the ratios of band intensities of *ura4*$^{+}$ integrated at outer repetitive region of centromere (*cen*) to euchromatic region (*DS/E*) signals in the ChIP DNA against those of input as measured by multiplex PCR. For average gene profiling shown in fig. S6, ORFs were divided into 30 equally sized segments. Geometric averages of the corresponding segments between ORFs were calculated and plotted as average enrichments over a 50bp region. 0 in X-axis represents the beginning of the ORF, and 1500 bp represents the end of the ORF. Y axis shows the average enrichments in log2 scale. Microarray

data are available at the US National Center for Biotechnology Information Gene Expression Omnibus (NCBI GEO) under the accession numbers GSE26999 and GSE17271.

Cross-correlation matrix and cluster analysis

For cross-correlation matrix and cluster analysis (Fig. 4C), median antisense ratios (mutant/WT) for 842 genes were calculated for each expression dataset. Linear regression analysis was performed between data sets, and Pearson-correlation index (*r*) was calculated. *r* value were converted into color codes and plotted as a matrix. Cluster analysis was performed according to the Euclidean distance of the *r* values between mutant strains.

Immunoprecipitation, protein purification and mass spectrometry

Flag-tagged Mlo3 and Cid14 were purified as described previously (*6*). Mlo3-HA immunoprecipitation was performed using the same protocol. Purified samples were either resolved by SDS-PAGE and visualized by Brilliant Blue staining or subjected to tandem MS (LC-MS/MS) analyses. Western blot analyses of purified samples was performed by using rabbit anti-HA (Abcam), Flag M2 (Sigma), anti-Penta-His (Molecular Probes), anti-Chp1 (Abcam) and rabbit anti-Myc (A-14, Santa Cruz). A longer exposure time was used to obtain the image shown for the anti-Flag (Fig. 1A) or anti-Myc (fig. S1) input blot compared to that of IP blot. For performing the RNase/DNase treatment shown in Fig. 4B, the immunoprecipitated samples were treated with or without 20ug of RNaseA/H mixture and/or 33ug DNase I before the final wash as indicated. The mass spectrometry analysis was performed as described previously (*3*). In brief, the tryptic peptides from each SDS-PAGE gel band were analyzed by a nano-capillary HPLC system (Agilent 1100, Agilent Technologies) with a 10 cm integrated μRPLC-electrospray ionization (ESI) emitter columns (made in house), coupled online with an linear ion-trap (IT) mass spectrometer (LTQ XP, Thermo Fisher Scientific). The peptides were eluted using a linear gradient 2% mobile phase B (acetonitrile with 0.1% formic acid) to 42% mobile phase B within 40 min at a constant flow rate of 250 nL/min. The seven most intense molecular ions in the MS scan were sequentially selected for subsequent collision-induced dissociation (CID) using a normalized collision energy of 35%. The ion source capillary voltage and temperature were set at 1.7 kV and 200 °C, respectively. The MS/MS data were searched against UniProt *S. pombe* database

from the European Bioinformatics Institute (http://www.ebi.ac.uk/integr8) using BioWorks interfaced SEQUEST (Thermo Fisher Scientific). Methionine oxidation (15.99) was searched as differential modifications. Up to two missed cleavage sites were allowed during the database search. The cut-off for legitimate identifications were charge state dependent cross correlation (X_{corr}) ≥ 2.0 for $[M+H]^{1+}$, ≥ 2.5 for $[M+2H]^{2+}$ and ≥ 3.0 for $[M+3H]^{3+}$ with delta correlation (ΔC_n) ≥ 0.10.

RNA analysis

Northern Blot was performed as previously described (*3*). Northern Blot for siRNA detection was carried out as previously described (*7*). Strand specific RT-PCRs were performed using centromeric primers as reported (*8*).

References:

1. A. G. Thakurta, G. Gopal, J. H. Yoon, L. Kozak, R. Dhar, *EMBO J.* **24**, 2512 (2005).
2. S. Jia, R. Kobayashi, S. I. Grewal, *Nat. Cell Biol.* **7**, 1007 (2005).
3. M. Zofall *et al.*, *Nature* **461**, 419 (2009).
4. J. Nakayama, J. C. Rice, B. D. Strahl, C. D. Allis, S. I. Grewal, *Science* **292**, 110 (2001).
5. H. P. Cam *et al.*, *Nat. Genet* **37**, 809 (2005).
6. K. Zhang, K. Mosch, W. Fischle, S. I. Grewal, *Nat. Struct. Mol. Biol.* **15**, 381 (2008).
7. T. Sugiyama *et al.*, *Cell* **128**, 491 (2007).
8. T. A. Volpe *et al.*, *Science* **297**, 1833 (2002).